Analytic expression for the giant fieldlike spin torque in spin-filter magnetic tunnel junctions

Y.-H. Tang,* Z.-W. Huang, and B.-H. Huang
Department of Physics, National Central University, Jung-Li 32001, Taiwan
(Received 26 March 2017; published 24 August 2017)

We propose analytic expressions for fieldlike, $T_\perp$, and spin-transfer, $T_\parallel$, spin torque components in the spin-filter-based magnetic tunnel junction (SFMTJ), by using the single-band tight-binding model with the nonequilibrium Keldysh formalism. In consideration of multireflection processes between noncollinear magnetization of the spin-filter (SF) barrier and the ferromagnetic (FM) electrode, the central spin-selective SF barrier plays an active role in the striking discovery $T_\perp \gg T_\parallel$, which can be further identified by the unusual barrier thickness dependence of giant $T_\perp$. Our general expressions reveal the sinusoidal angular dependence of both spin torque components, even in the presence of the SF barrier.

DOI: 10.1103/PhysRevB.96.064429

Recently, there has been much attention on exploring spin-dependent transport in magnetic tunnel junctions (MTJs) [1,2], especially new phenomena such as nonvolatile magnetic random access memory (MRAM), in which a magnetic state can be controlled either by an external magnetic field via the tunnel magnetoresistance (TMR) effect [3–5] or a sufficiently large current to induce the spin torque effect [6–9]. In conventional ferromagnetic/nonmagnetic insulator/ferromagnetic (FM/I/FM) MTJs, the spin-polarized current arises from the spin imbalance of the spin-up and spin-down densities of states of conduction electrons at the Fermi energy in a FM electrode. The spin-filter-based magnetic tunnel junction (SFMTJ), on the other hand, has emerged as a promising alternative for generating a highly spin-polarized current via the exchange splitting between spin-up and spin-down conduction bands of a spin-filter (SF) barrier.

A lot of effort has been devoted to studying the spin-filtering effect of ferromagnetic insulators [10–15], which are unique in that they are magnetically active due to the spins of localized electrons but electrically inactive with frozen charge degrees of freedom. The TMR effect has been experimentally observed in nonmagnetic metal/SF/FM (NM/SF/I/FM) [16,17], NM/SF/I/SF/NM [18,19], and FM/SF/FM MTJs [20,21], where the resistance of the junction strongly depends on the relative magnetization orientation between SF barrier and FM electrode. However, only a few theoretical works have been developed to investigate the spin torque effect for SFMTJs in the noncollinear magnetic configuration [22–24]. Recently, Tang *et al.* [24] proposed a dual manipulation of $T_\perp$ either via external magnetic field or external bias, which provides a promising avenue for achieving both reading and writing processes of nonvolatile fieldlike spin torque MRAM (FLST-MRAM).

In this work, the multireflection processes of central I/SF/I tribarriers are taken into account in the analytic formulations of fieldlike ($T_\perp$) and spin-transfer ($T_\parallel$) components of spin torque in FM/I/SF/I/FM SFMTJs. We employ the single-band tight-binding model with the nonequilibrium Keldysh formalism to derive exact and general expressions of both spin torque components, which suggests their sinusoidal angular dependence even in the presence of a SF barrier. The unusual barrier thickness dependence of $T_\perp$ is proposed to elucidate the underlying mechanism of SF-assisted enhancement of $T_\perp$ in terms of substantial spin-dependent multireflection at SF/I interfaces.

The FM/I/SF/I/FM junction, shown schematically in Fig. 1, consists of semi-infinite left and right FM electrodes sandwiching the central region of the three-layer I/SF/I barrier. To prevent direct exchange coupling between $\mathbf{M_{SF}}$ and $\mathbf{M_L}$ ($\mathbf{M_R}$), a nonmagnetic insulating (I) layer serves as spacer between SF and FM electrode. $N_{IL,SF,IR}$ denotes the number of left-I, SF, and right-I layers, respectively. The magnetization of the left (fixed) FM electrode, $\mathbf{M_L}$, and the central FM barrier, $\mathbf{M_{SF}}$, are pinned along the z direction, while that of the right (free) FM electrode, $\mathbf{M_R}$, is rotated by an angle θ around the y axis with respect to $\mathbf{M_L}$ to form parallel (PC, $\theta = 0$) and antiparallel (APC, $\theta = \pi$) magnetic configurations.

The single-orbital simple cubic tight-binding Hamiltonian [25–27] for the FM/I/SF/I/FM junction can be expressed as $H = H_L + H_R + H_{IL} + H_{SF} + H_{IR} + H_{cpl}$, where H_L, H_R, H_{IL}, H_{IR}, and H_{SF} are the Hamiltonian of isolated left and right electrodes, left- and right-I barriers, and central SF barriers, respectively, and H_{cpl} involves the couplings between two neighboring regions. To simulate the real $Co/Al_2O_3/EuS/Al_2O_3/Co$ junction, we choose the spin-polarized on-site energies of SF, I, and FM regions as $\varepsilon_{SF}^{\uparrow(\downarrow)} = 5.78\ \text{eV} \mp \Delta$, $\varepsilon_I = 5.98$ eV, and $\varepsilon^{\uparrow(\downarrow)} = 1.0$ eV (2.5 eV), respectively, and the nearest-neighbor hopping matrix element is $t = -0.83$ eV in all regions. The exchange splitting of FM electrode is defined by $\delta = \varepsilon^{\downarrow} - \varepsilon^{\uparrow}$. These energy parameters are based on the insulating barrier height $\varphi_I = 1.0$ eV, the average SF barrier height $\varphi_0 = 0.8$ eV, and the exchange field $\Delta = 0.12$ eV in $Al/EuS/Al_2O_3/Co$ junction [17].

When SFMTJ is under an external bias, V, the chemical potential of right FM electrode is shifted with respect to that of left FM electrode by $\mu_R - \mu_L = \text{eV}$, and μ_L is fixed at the Fermi energy, $E_F = 0.0$ eV. Here we define that spin-polarized current flows along the y direction, and hence the spin current density accumulated at the right I/FM interface can be obtained by the nonequilibrium Keldysh formalism [27,28],

$$Q_{iy} = \frac{t}{16\pi^3} \int \mathrm{Tr}[(\hat{G}^<_{\alpha' b} - \hat{G}^<_{b\alpha'})\sigma_i] dE d\mathbf{k}_\parallel, \qquad (1)$$

*yhtang@cc.ncu.edu.tw

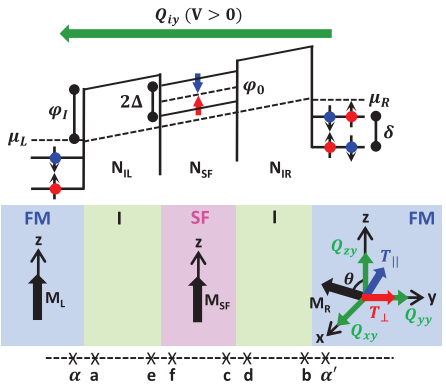

FIG. 1. Schematic of energy profile for FM/I/SF/I/FM junction, consisting of two nonmagnetic insulating (I) layers between semi-infinite FM electrode and SF layers, in noncollinear magnetic configuration. $N_{IL,SF,IR}$ denotes the numbers of left-I, SF, and right-I layers, respectively. The magnetization of the left (fixed) FM, $\mathbf{M_L}$, and of the SF barrier, $\mathbf{M_{SF}}$, are pinned along the z direction, while that of the right (free) FM, $\mathbf{M_R}$, is rotated by an angle θ around the y axis with respect to $\mathbf{M_L}$. The spin-polarized current densities, Q_{iy}, where $i = x,y,z$, flow from right to left for a positive bias. The net fieldlike, $T_\perp$, and spin-transfer, $T_\parallel$, components of spin torque on the right FM electrode are along $\hat{\mathbf{M}}_\mathbf{L} \times \hat{\mathbf{M}}_\mathbf{R}$ and $\hat{\mathbf{M}}_\mathbf{R} \times (\hat{\mathbf{M}}_\mathbf{L} \times \hat{\mathbf{M}}_\mathbf{R})$ directions, respectively.

where i denotes the spin direction, $\sigma = (\sigma_x,\sigma_y,\sigma_z)$ is the vector of the 2×2 Pauli matrix, $\mathbf{k}_\parallel$ is the transverse component of the wave vector, and the energy integral is over occupied states. Following the theoretical work in a double-barrier magnetic tunnel junction [29], we can calculate Q_{iy} directly by solving the tight-binding Hamiltonian. On the other hand, we further propose analytic derivations of Q_{iy} to better understand the sinusoidal angular and the unusual barrier thickness dependence of spin torque effect in SFMTJs as follows.

The 2×2 Keldysh Green's function matrix in spin space between the last site of the right-I barrier (b site) and the first site of the right FM electrode (α' site) is defined by the Dyson equation,

$$\begin{aligned}
\hat{G}^<_{\alpha' b} &= \hat{g}^r_{\alpha'\alpha'} t \hat{G}^<_{bb} + \hat{g}^<_{\alpha'\alpha'} t \hat{G}^a_{bb},\\
\hat{G}^<_{b\alpha'} &= \hat{G}^r_{bb} t \hat{g}^<_{\alpha'\alpha'} + \hat{G}^<_{bb} t \hat{g}^a_{\alpha'\alpha'},\\
\hat{G}^<_{bb} &= \hat{G}^r_{ba} t \hat{g}^<_{\alpha\alpha} t \hat{G}^a_{ab} + \hat{G}^r_{bb} t \hat{g}^<_{\alpha'\alpha'} t \hat{G}^a_{bb},
\end{aligned} \tag{2}$$

where $\hat{g}^{r,a,<}$ and $\hat{G}^{r,a,<}$ are the retarded, advanced, and Keldysh Green's functions of each uncoupled region and the coupled system, respectively, and the subscripts refer to the sites in various regions of FM/I/SF/I/FM junction as shown in Fig. 1. In the limit of the thick barrier [27], we can obtain

$$\hat{G}^a_{ab} \sim t^2 g_{bd} \hat{g}_{cf} g_{ea} \tag{3}$$

and

$$\hat{G}^r_{bb} = g_{bb} + \hat{G}^{SF1}_{bb} + \hat{G}^{SF2}_{bb} + \hat{G}^I_{bb} + O(t^8). \tag{4}$$

Due to the noncollinear configuration between $\mathbf{M_R}(\theta)$ and $\mathbf{M_{SF(L)}}$, here we only consider the first eight terms of $\hat{G}^r_{bb}$

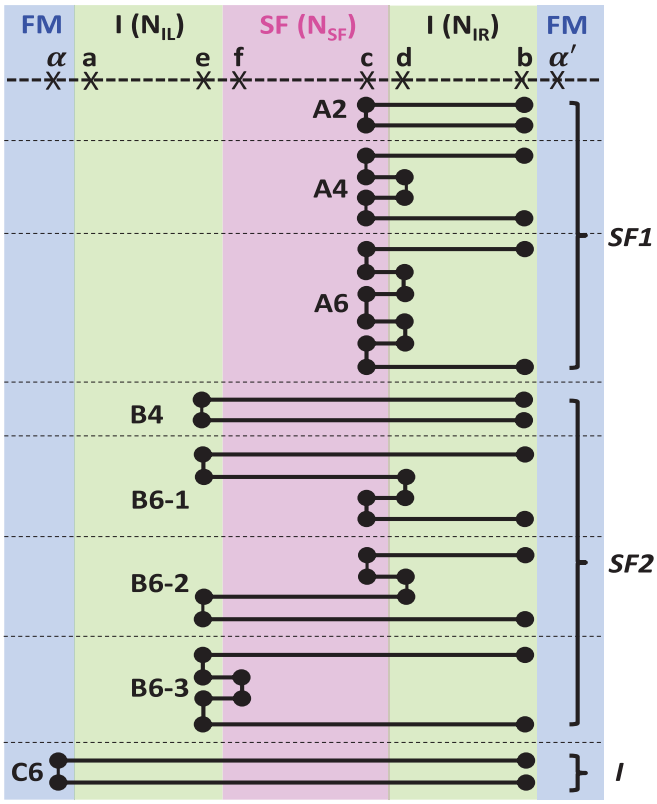

FIG. 2. Schematic of the first eight terms of $\hat{G}^r_{bb}$ in FM/I/SF/I/FM junction to include the multireflection at SF/I interfaces (A2, A4, A6, B4, B6-1, B6-2, and B6-3) and the direct transport through whole junction (C6). These terms can be divided into three groups, i.e., $SF1$, $SF2$, and I.

expanded in the power of t as shown in Fig. 2, which can be divided into three groups as

$$\begin{aligned}
\hat{G}^{SF1}_{bb} &= \hat{G}^{A2}_{bb} + \hat{G}^{A4}_{bb} + \hat{G}^{A6}_{bb}\\
&\sim |\, g_{db} \,|^2 \begin{bmatrix} t^2 \hat{g}_{cc} \\ +t^4 \,|\, \hat{g}_{cc} \,|^2\, g_{dd} \\ +t^6 \,|\, \hat{g}_{cc} \,|^3 |\, g_{dd} \,|^2 \end{bmatrix},
\end{aligned} \tag{5}$$

$$\begin{aligned}
\hat{G}^{SF2}_{bb} &= \hat{G}^{B4}_{bb} + \hat{G}^{B6-1}_{bb} + \hat{G}^{B6-2}_{bb} + \hat{G}^{B6-3}_{bb}\\
&\sim |\, g_{db} \,|^2 |\, \hat{g}_{fc} \,|^2 \begin{bmatrix} t^4 g_{ee} \\ +2t^6 g_{ee} \hat{g}_{cc} g_{dd} \\ +t^6 \,|\, g_{ee} \,|^2\, \hat{g}_{ff} \end{bmatrix},
\end{aligned} \tag{6}$$

$$\hat{G}^I_{bb} = \hat{G}^{C6}_{bb} \sim t^6 \,|\, g_{db} \,|^2 |\, \hat{g}_{fc} \,|^2 |\, g_{ae} \,|^2\, \hat{g}^r_{\alpha\alpha}. \tag{7}$$

Here the uncoupled Green's functions of the isolated nonmagnetic I barrier, g_{ae}, g_{db}, g_{ee}, g_{dd}, and g_{bb}, are real numbers.

By substituting Eqs. (3)–(7) into Eq. (2), the Keldysh Green's function at the right I/FM interface can be written as

$$\hat{G}^<_{\alpha' b} - \hat{G}^<_{b\alpha'} = \hat{G}^I + \hat{G}^{SF1} + \hat{G}^{SF2}. \tag{8}$$

Analogous to Eq. (9) in Ref. [27] for the conventional FM/I/FM junction, $\hat{G}^I$ is the Keldysh Green's function for the electrons

tunneling through entire FM/I/SF/I/FM junction,

$$\hat{G}^{I} \sim t^{7} \mid g_{ae} \mid^{2} \mid g_{db} \mid^{2} \times \begin{bmatrix} \hat{g}^{r}_{\alpha'\alpha'}\hat{g}_{cf}\hat{g}^{<}_{\alpha\alpha}\hat{g}_{fc} \\ +\hat{g}^{<}_{\alpha'\alpha'}\hat{g}_{cf}\hat{g}^{a}_{\alpha\alpha}\hat{g}_{fc} \\ -\hat{g}_{cf}\hat{g}^{<}_{\alpha\alpha}\hat{g}_{fc}\hat{g}^{a}_{\alpha'\alpha'} \\ -\hat{g}_{cf}\hat{g}^{r}_{\alpha\alpha}\hat{g}_{fc}\hat{g}^{<}_{\alpha'\alpha'} \end{bmatrix}. \tag{9}$$

The additional two terms, $\hat{G}^{SF1}$ and $\hat{G}^{SF2}$, arise from the spin-dependent multireflection at two SF/I interfaces due to the electrons injected solely from right FM electrode,

$$\hat{G}^{SF1} \sim t^{3} \mid g_{db} \mid^{2} \times \begin{bmatrix} \hat{g}^{<}_{\alpha'\alpha'}\hat{g}_{cc} - \hat{g}_{cc}\hat{g}^{<}_{\alpha'\alpha'} \\ +t^{2} g_{dd}\left(\hat{g}^{<}_{\alpha'\alpha'} \mid \hat{g}_{cc} \mid^{2} - \mid \hat{g}_{cc} \mid^{2} \hat{g}^{<}_{\alpha'\alpha'}\right) \\ +t^{4} \mid g_{dd} \mid^{2} \left(\hat{g}^{<}_{\alpha'\alpha'} \mid \hat{g}_{cc} \mid^{3} - \mid \hat{g}_{cc} \mid^{3} \hat{g}^{<}_{\alpha'\alpha'}\right) \end{bmatrix} \tag{10}$$

and

$$\hat{G}^{SF2} \sim t^{5} \mid g_{db} \mid^{2} \times \begin{bmatrix} g_{ee}\left(\hat{g}^{<}_{\alpha'\alpha'} \mid \hat{g}_{fc} \mid^{2} - \mid \hat{g}_{fc} \mid^{2} \hat{g}^{<}_{\alpha'\alpha'}\right) \\ +2t^{2} g_{ee} g_{dd}\left(\hat{g}^{<}_{\alpha'\alpha'} \mid \hat{g}_{fc} \mid^{2} \hat{g}_{cc} - \mid \hat{g}_{fc} \mid^{2} \hat{g}_{cc}\hat{g}^{<}_{\alpha'\alpha'}\right) \\ +t^{2} \mid g_{ee} \mid^{2} \left(\hat{g}^{<}_{\alpha'\alpha'} \mid \hat{g}_{fc} \mid^{2} \hat{g}_{ff} - \mid \hat{g}_{fc} \mid^{2} \hat{g}_{ff}\hat{g}^{<}_{\alpha'\alpha'}\right) \end{bmatrix}, \tag{11}$$

where $\hat{g}^{<}_{\alpha\alpha(\alpha'\alpha')} = -2if_{L(R)}Im\{\hat{g}^{r}_{\alpha\alpha(\alpha'\alpha')}\}$ and $f_{L(R)}$ is the Fermi-Dirac distribution function of left (right) FM electrode.

Since $\mathbf{M_L}$ and $\mathbf{M_{SF}}$ are pinned along the z direction and $\mathbf{M_R}$ is rotated by an angle θ around the y axis with respect to $\mathbf{M_L}$, the 2×2 retarded surface Green's function matrices in spin space for the isolated left and right FM electrodes can be written as

$$\hat{g}^{r}_{\alpha\alpha} = \begin{pmatrix} g^{\uparrow}_{L} & 0 \\ 0 & g^{\downarrow}_{L} \end{pmatrix}; \quad \hat{g}_{fc,cc,ff} = \begin{pmatrix} g^{\uparrow}_{fc,cc,ff} & 0 \\ 0 & g^{\downarrow}_{fc,cc,ff} \end{pmatrix} \tag{12}$$

and

$$\hat{g}^{r}_{\alpha'\alpha'} = \begin{pmatrix} g^{\uparrow\uparrow}_{\alpha'\alpha'} & g^{\uparrow\downarrow}_{\alpha'\alpha'} \\ g^{\downarrow\uparrow}_{\alpha'\alpha'} & g^{\downarrow\downarrow}_{\alpha'\alpha'} \end{pmatrix}, \tag{13}$$

where

$$\begin{aligned} g^{\uparrow\uparrow}_{\alpha'\alpha'} &= g^{\uparrow}_{R}\cos^{2}(\theta/2) + g^{\downarrow}_{R}\sin^{2}(\theta/2), \\ g^{\downarrow\downarrow}_{\alpha'\alpha'} &= g^{\uparrow}_{R}\sin^{2}(\theta/2) + g^{\downarrow}_{R}\cos^{2}(\theta/2), \\ g^{\uparrow\downarrow(\downarrow\uparrow)}_{\alpha'\alpha'} &= \sin\theta\left(g^{\uparrow}_{R} - g^{\downarrow}_{R}\right)/2. \end{aligned} \tag{14}$$

Here $g^{\uparrow,\downarrow}_{L(R)}$ are complex numbers for the FM electrode, and $g^{\uparrow,\downarrow}_{fc,cc,ff}$ are real numbers for the SF barrier.

The net fieldlike, $T_{\perp}$, component of spin torque on the right FM electrode, which is along the $\hat{\mathbf{M}}_{\mathbf{L}} \times \hat{\mathbf{M}}_{\mathbf{R}}$ direction as shown in Fig. 1, can be simply expressed by the spin current density accumulation at right I/FM interface per unit area, $\square$ [25],

$$T_{\perp} = Q_{yy}. \tag{15}$$

By substituting Eq. (8) into Eq. (1), the three nonzero $\mathrm{Im}\{\hat{G}^{I}\}$, $\mathrm{Im}\{\hat{G}^{SF1}\}$, and $\mathrm{Im}\{\hat{G}^{SF2}\}$ terms all contribute to $T_{\perp}$,

$$T_{\perp} = T^{I}_{\perp} + T^{SF1}_{\perp} + T^{SF2}_{\perp}. \tag{16}$$

These three components in noncollinear magnetic configuration can be expressed in the general forms of

$$T^{I,SF1,SF2}_{\perp}(\theta) = \sin\theta \begin{bmatrix} J^{I,SF1,SF2}_{\uparrow\uparrow} + J^{I,SF1,SF2}_{\downarrow\downarrow} \\ -J^{I,SF1,SF2}_{\uparrow\downarrow} - J^{I,SF1,SF2}_{\downarrow\uparrow} \end{bmatrix}, \tag{17}$$

where

$$J^{I}_{\sigma\sigma'} \approx \frac{-t^{8}}{8\pi^{3}} \int dE d\mathbf{k}_{\parallel} \mid g_{I} \mid^{4} \times \begin{bmatrix} f_{R}(E-eV)\mathrm{Re}\{g^{\sigma}_{L}\} \mid g^{\sigma}_{SF} \mid^{2} \mathrm{Im}\{g^{\sigma'}_{R}\} \\ +f_{L}(E)\mathrm{Im}\{g^{\sigma}_{L}\} \mid g^{\sigma}_{SF} \mid^{2} \mathrm{Re}\{g^{\sigma'}_{R}\} \end{bmatrix}, \tag{18}$$

$$J^{SF1}_{\sigma\sigma'} \approx \frac{-t^{4}}{8\pi^{3}} \int dE d\mathbf{k}_{\parallel} \mid g_{I} \mid^{2} f_{R}(E-eV)\mathrm{Im}\{g^{\sigma'}_{R}\} \times [g^{\sigma}_{cc} + t^{2} g_{dd} \mid g^{\sigma}_{cc} \mid^{2} + t^{4} \mid g_{dd} \mid^{2} \mid g^{\sigma}_{cc} \mid^{3}], \tag{19}$$

and

$$J^{SF2}_{\sigma\sigma'} \approx \frac{-t^{6}}{8\pi^{3}} \int dE d\mathbf{k}_{\parallel} \mid g_{I} \mid^{2} f_{R}(E-eV)\mathrm{Im}\{g^{\sigma'}_{R}\} \times \mid g^{\sigma}_{SF} \mid^{2} [g_{ee} + 2t^{2} g_{ee} g_{dd} g^{\sigma}_{cc} + t^{2} \mid g_{ee} \mid^{2} g^{\sigma}_{ff}]. \tag{20}$$

Here we denote $g_{I} = g_{db} = g_{ae}$ for isolated nonmagnetic I barrier and $g^{\sigma}_{SF} = g^{\sigma}_{fc}$ for σ-spin state of isolated SF barrier. The $J_{\sigma\sigma'}$ is the nonequilibrium interlayer exchange coupling (NEIEC) between the σ-spin state of the left FM electrode and the σ'-spin state of the right FM electrode via the σ-spin state of central SF barrier in the PC case. We can further replace $J_{\uparrow\uparrow(\downarrow\downarrow)}$ and $J_{\uparrow\downarrow(\downarrow\uparrow)}$ by $J_{\uparrow(\downarrow)}(PC)$ and $J_{\uparrow(\downarrow)}(APC)$, respectively, since in the APC case we simply exchange spin-$\uparrow$ and spin-$\downarrow$ energy states of right FM electrode. Thus, Eq. (17) is consistent with Eq. (5) of Ref. [24].

It is worthwhile to emphasize that $T^{SF1}_{\perp}$ and $T^{SF2}_{\perp}$ can be either understood by the NEIEC's between noncollinear $\mathbf{M_R}(\theta)$ in right FM electrode and $\mathbf{M_{SF}}$ in SF barrier, or explained by the spin current accumulation from those incoming electrons solely from right FM electrode encountering multireflection processes at SF/I interfaces. $T^{I}_{\perp}$ is similar to that in the conventional I-based MTJs [30], simply resulting from the NEIECs between noncollinear $\mathbf{M_R}(\theta)$ and $\mathbf{M_L}$.

The net spin-transfer, $T_{\parallel}$, component of spin torque on the right FM electrode, which is along the $\hat{\mathbf{M}}_{\mathbf{R}} \times (\hat{\mathbf{M}}_{\mathbf{L}} \times \hat{\mathbf{M}}_{\mathbf{R}})$ direction as shown in Fig. 1, is defined by

$$T_{\parallel} = -Q_{xy}\cos\theta + Q_{zy}\sin\theta. \tag{21}$$

After we substitute Eq. (8) into Eq. (1), unlike $T_{\perp}$, only the contribution from $\mathrm{Re}\{\hat{G}^{I}\}$ exists while those from $\mathrm{Re}\{\hat{G}^{SF1}\}$

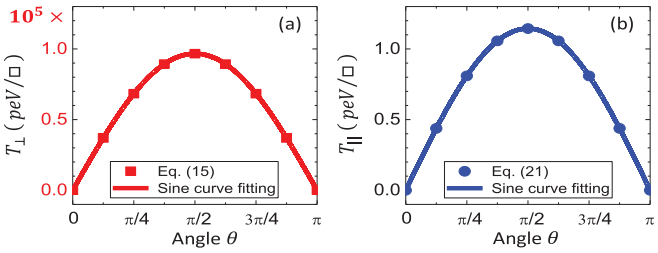

FIG. 3. The angular dependence of (a) $T_\perp$ and (b) $T_\parallel$ for SFMJ with $N_{IL} = N_{SF} = N_{SF} = 3$ and an external bias of 0.2 V. The solid points are calculated by exact formalisms of Eqs. (15) and (21), and the solid lines are the sine curve fitting.

and $\mathrm{Re}\{\hat{G}^{SF2}\}$ vanish. The noncollinear $T_\parallel(\theta)$ can be either written as

$$\begin{aligned} T_\parallel(\theta) &= T_\parallel^I(\theta) \\ &\approx \frac{-t^8\sin\theta}{8\pi^3}\int [f_R(E-eV)-f_L(E)]\times \mid g_I \mid^4 \\ &\times [\mathrm{Im}\{g_L^\uparrow\} \mid g_{SF}^\uparrow \mid^2 -\mathrm{Im}\{g_L^\downarrow\} \mid g_{SF}^\downarrow \mid^2] \\ &\times [\,\mathrm{Im}\{g_R^\uparrow\}+\mathrm{Im}\{g_R^\downarrow\}]dEd\mathbf{k}_\parallel, \end{aligned} \tag{22}$$

or recast in the general form of

$$T_\parallel(\theta) = \frac{-\sin\theta}{2}\left[I_z^{(s)}(PC)+I_z^{(s)}(APC)\right]. \tag{23}$$

The spin current densities along the z direction, $I_z^{(s)} = \hbar(I^\uparrow - I^\downarrow)/2e$, at the right I/FM interface in PC and APC cases can be obtained by substituting Eq. (8) into Q_{zy} of Eq. (1),

$$\begin{aligned} I_z^{(s)}(PC,APC) \approx \frac{t^8}{4\pi^3}\int [f_R(E-eV)-f_L(E)]\times \mid g_I \mid^4 \\ \times\begin{bmatrix} \mid g_{SF}^\uparrow \mid^2 \mathrm{Im}\{g_L^\uparrow\}\mathrm{Im}\{g_R^{\uparrow,\downarrow}\} \\ -\mid g_{SF}^\downarrow \mid^2 \mathrm{Im}\{g_L^\downarrow\}\mathrm{Im}\{g_R^{\downarrow,\uparrow}\} \end{bmatrix} dEd\mathbf{k}_\parallel. \end{aligned} \tag{24}$$

In Figs. 3(a) and 3(b), we present the sinusoidal angular behaviors of both $T_\perp$ and $T_\parallel$ in noncollinear SFMJ with $N_{IL} = N_{SF} = N_{IR} = 3$ and an external bias of 0.2 V, which agree with our derived general expressions in Eqs. (17) and (23), respectively. In sharp contrast to the fact of $T_\perp \ll T_\parallel$ in conventional I-based MTJs [31], we predict the giant value of $T_\perp$, which is about five orders larger than that of $T_\parallel$ in SFMTJ. Such an intriguing finding may provide a promising solution to efficiently reduce the writing current densities in MRAM applications.

To further elucidate the underlying mechanism of SF-assisted significant enhancement of $T_\perp$, we investigate the barrier thickness dependence of both spin torque components in SFMTJ. Since $T_\perp^{SF1,SF2,I}(\theta=\pi/2)$ and $T_\parallel(\theta=\pi/2)$ of SFMTJ all exhibit exponential decay with barrier thickness, $d = Na$, where $N = (N_{IL}, N_{SF}, N_{IR})$, we can recast them in

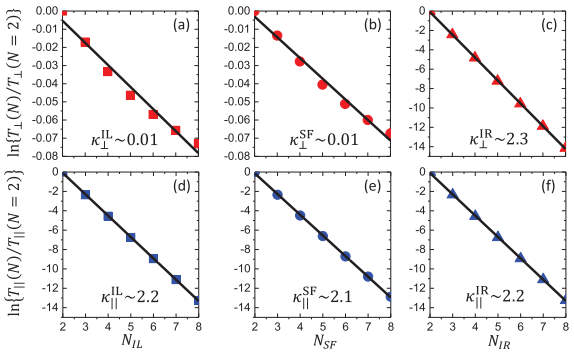

FIG. 4. Barrier thickness dependence of $\ln\{T_\perp(\theta=\pi/2)\}$ normalized to its value for the two-layer thickness in SFMJs with (a) (N_{IL},3,3), (b) (3,N_{SF},3), and (c) (3,3,N_{IR}) and of $\ln\{T_\parallel(\theta=\pi/2)\}$ normalized to its value for the two-layer thickness in SFMJs with (d) (N_{IL},3,3), (e) (3,N_{SF},3), and (f) (3,3,N_{IR}). An external bias of 0.2 V is applied. $\kappa_{IL,SF,IR}$ denote the fitted decay rates within left-I, SF, and right-I barriers, respectively.

the forms of

$$\begin{bmatrix} T_\perp^{SF1} \\ T_\perp^{SF2} \\ T_\perp^{I} \end{bmatrix} = \begin{bmatrix} A^{SF1}e^{-\kappa_\perp^{IR}N_{IR}a} \\ A^{SF2}e^{-\kappa_\perp^{SF}N_{SF}a}e^{-\kappa_\perp^{IR}N_{IR}a} \\ A^{I}e^{-\kappa_\perp^{IL}N_{IL}a}e^{-\kappa_\perp^{SF}N_{SF}a}e^{-\kappa_\perp^{IR}N_{IR}a} \end{bmatrix} \tag{25}$$

and

$$T_\parallel = B^I e^{-\kappa_\parallel^{IL}N_{IL}a}e^{-\kappa_\parallel^{SF}N_{SF}a}e^{-\kappa_\parallel^{IR}N_{IR}a}, \tag{26}$$

where a is the cubic unit cell length in our tight-binding model. A^I and B^I are related to the tunneling probability through the whole junction, and $A^{SF1,SF2}$ can be correlated with the multireflection probability at SF/I interfaces. The decay rates of $T_\perp$ and $T_\parallel$ within left-I, SF, and right-I barriers can be simply estimated by the slops of linear regression to the $\ln\{T_{\perp,\parallel}(N)/T_{\perp,\parallel}(N=2)\}$ versus $N = (N_{IL}, N_{SF}, N_{IR})$ plots as shown in Fig. 4. Surprisingly, our results reveal an unusual barrier thickness dependence of $T_\perp$ with $\kappa_\perp^{IR} \gg \kappa_\perp^{SF} \sim \kappa_\perp^{IL}$. Since $T_\perp^{SF1}$ only depends on N_{IR} but is nearly independent of N_{SF} and N_{IL}, the strong (weak) decay of $T_\perp$ with N_{IR} ($N_{IL,SF}$) reveals that $T_\perp^{SF1}$ much outweighs $T_\perp^{SF2,I}$ and thus dominates the giant value of $T_\perp$. This can be understood by the significant NEIEC's between noncollinear $\mathbf{M_R}(\theta)$ and $\mathbf{M_{SF}}$ via the spin-dependent multireflection processes at SF/I interfaces. On the other hand, the large decay rates of $T_\parallel$ within all three barriers in SFMTJs are similar to those in conventional I-based MTJs, since $T_\parallel = T_\parallel^I$ is only related to the spin current through whole tunneling junction between PC and APC cases.

In conclusion, analytic expressions are proposed to investigate how the spin-selective SF barrier affects both components of spin torque in the FM/I/SF/I/FM junction, by using the single-band tight-binding model with the nonequilibrium Keldysh formalism. Our newly derived general expressions suggest the sinusoidal angular behaviors of both components of spin torque even in the presence of a central SF barrier. In consideration of multireflection processes at SF/I interfaces, we predict an intriguing finding of $T_\perp \gg T_\parallel$, which is in sharp contrast to the small value of $T_\perp$ in

conventional MTJs with nonmagnetic I barrier. Due to the unusual barrier thickness dependence of giant $T_\perp$, the $T_\perp^{SF1}$ dominates the SF-assisted giant value of $T_\perp$ but gives no contribution to $T_\parallel$. Our theoretical works may serve as simple guiding rules for nonvolatile fieldlike spin-torque-based MRAM (FLST-MRAM) by manipulating giant $T_\perp$ with lower current density.

ACKNOWLEDGMENTS

This work is supported by the Ministry of Science and Technology (NSC 102-2112-M-008-004-MY3 and MOST 105-2112-M-008-010-) and the National Center of Theoretical Science, Republic of China.

[1] I. Žutić, J. Fabian, and S. D. Sarma, Rev. Mod. Phys. **76**, 323 (2004).
[2] G.-X. Miao, M. Munzenberg, and J. S. Moodera, Rep. Prog. Phys. **74**, 036501 (2011).
[3] M. Julliere, Phys. Lett. A **54**, 225 (1975).
[4] S. S. P. Parkin, C. Kaiser, A. Panchula, P. M. Rice, B. Hughes, M. Samant, and S.-H. Yang, Nat. Mater. **3**, 862 (2004).
[5] S. Yuasa, T. Nagahama, A. Fukushima, Y. Suzuki, and K. Ando, Nat. Mater. **3**, 868 (2004).
[6] J. C. Slonczewski, Phys. Rev. B **39**, 6995 (1989).
[7] L. Berger, Phys. Rev. B **54**, 9353 (1996).
[8] H. Kubota, A. Fukushima, K. Yakushiji, T. Nagahama, S. Yuasa, K. Ando, H. Maehara, Y. Nagamine, K. Tsunekawa, D. D. Djayaprawira, N. Watanabe, and Y. Suzuki, Nat. Phys. **4**, 37 (2008).
[9] C. Wang, Y.-T. Cui, J. A. Katine, R. A. Buhrman, and D. C. Ralph, Nat. Phys. **7**, 496 (2011).
[10] J. S. Moodera, X. Hao, G. A. Gibson, and R. Meservey, Phys. Rev. Lett. **61**, 637 (1988).
[11] J. S. Moodera, R. Meservey, and X. Hao, Phys. Rev. Lett. **70**, 853 (1993).
[12] T. S. Santos and J. S. Moodera, Phys. Rev. B **69**, 241203(R) (2004).
[13] J. S. Moodera, G. X. Miao, and T. S. Santos, Phys. Today **63**, 46 (2010).
[14] U. Lüders, A. Barthélémy, M. Bibes, K. Bouzehouane, S. Fusil, E. Jacquet, J.-P. Contour, J.-F. Bobo, J. Fontcuberta, and A. Fert, Adv. Mater. **18**, 1733 (2006).
[15] S. Matzen, J.-B. Moussy, G. X. Miao, and J. S. Moodera, Phys. Rev. B **87**, 184422 (2013).
[16] P. LeClair, J. K. Ha, H. J. M. Swagten, J. T. Kohlhepp, C. H. van de Vin, and W. J. M. de Jonge, Appl. Phys. Lett. **80**, 625 (2002).
[17] T. Nagahama, T. S. Santos, and J. S. Moodera, Phys. Rev. Lett. **99**, 016602 (2007).
[18] G. X. Miao, M. Müller, and J. S. Moodera, Phys. Rev. Lett. **102**, 076601 (2009).
[19] G. X. Miao, J. Chang, B. A. Assaf, D. Heiman, and J. S. Moodera, Nat. Commun. **5**, 3682 (2014).
[20] B. Prasad, M. Egilmez, F. Schoofs, T. Fix, M. E. Vickers, W. Zhang, J. Jian, H. Wang, and M. G. Blamire, Nano Lett. **14**, 2789 (2014).
[21] B. Prasad and M. G. Blamire, Appl. Phys. Lett. **109**, 132407 (2016).
[22] J. I. Inoue, Phys. Rev. B **84**, 180402(R) (2011).
[23] C. Ortiz Pauyac, A. Kalitsov, A. Manchon, and M. Chshiev, Phys. Rev. B **90**, 235417 (2014).
[24] Y.-H. Tang, F.-C. Chu, and N. Kioussis, Sci. Rep. **5**, 11341 (2015).
[25] I. Theodonis, N. Kioussis, A. Kalitsov, M. Chshiev, and W. H. Butler, Phys. Rev. Lett. **97**, 237205 (2006).
[26] A. Kalitsov, M. Chshiev, I. Theodonis, N. Kioussis, and W. H. Butler, Phys. Rev. B **79**, 174416 (2009).
[27] Y.-H. Tang, N. Kioussis, A. Kalitsov, W. H. Butler, and R. Car, Phys. Rev. B **81**, 054437 (2010).
[28] C. Caroli, R. Combescot, P. Nozieres, and D. Saint-James, J. Phys. C: Solid St. Phys. **4**, 916 (1971).
[29] I. Theodonis, A. Kalitsov, and N. Kioussis, Phys. Rev. B **76**, 224406 (2007).
[30] Y.-H. Tang, N. Kioussis, A. Kalitsov, W. H. Butler, and R. Car, Phys. Rev. Lett. **103**, 057206 (2009).
[31] P. M. Haney, C. Heiliger, and M. D. Stiles, Phys. Rev. B **79**, 054405 (2009).